PNAS
www.pnas.org

Supplementary Information for

Perturbations in plant energy homeostasis prime lateral root initiation via SnRK1-bZIP63-ARF19 signalling

Prathibha Muralidhara, Christoph Weiste, Silvio Collani, Markus Krischke, Philipp Kreisz, Jan Draken, Regina Feil, Andrea Mair, Markus Teige, Martin J. Müller, Markus Schmid, Dirk Becker, John E. Lunn, Filip Rolland, Johannes Hanson, Wolfgang Dröge-Laser

Wolfgang Dröge-Laser and Christoph Weiste
Email: wolfgang.droege-laser@uni-wuerzburg.de; christoph.weiste@uni-wuerzburg.de

This PDF file includes:

Supplementary Methods

Root phenotyping

At 14 DAG, seedlings were scanned with a Plustek Opticbook 3600 plus scanner and primary root length was measured (in cm) from the end of the hypocotyl to the root tip by using the free-hand tool of Fiji (1). Macroscopically visible LRs (emerged LR) were counted on each plant and eLRD was calculated by dividing LR number by primary root length.

Overall root architecture was determined by generating outline images. Eight d-old WT and *bzip63* loss-of-function seedlings were grown on ½ MS media without sugars solidified with phytoagar and subjected to 4 h of uD. After dark treatment, they were placed back to long-day conditions and were imaged 14 DAG. An overlay image of 10 seedlings per genotype and condition was used to construct a maximum projection of the root system by marking the outermost root structures using the straight-line tool of MS PowerPoint.

Confocal imaging

To determine *GATA23* expression, 5 d-old transgenic p*GATA23*::NLS-GFP seedlings, grown on solidified ½ MS agar plates, were subjected to 4 h of uD and transferred back to long day regime. Control plants were constantly kept under long-day growth conditions. After a 16 h recovery phase, seedlings were imaged using a Leica SP5 confocal microscope at 25x magnification (emission at 488-507nm). The whole root, from root tip to hypocotyl was scanned and stacks of individual images for each part of the seedling were obtained and the entire primary root was reconstructed using image tiles in MS PowerPoint. Subsequently the number of LRs at different stages of development (stage I to stage VII) (2) were counted in both control and darkness treated seedlings.

To determine *bZIP63* expression domains 5 d-old *bzip63* mutant seedlings complemented with a Pro*bZIP63*:*bZIP63*:YFP construct were grown on ½ MS agar plates without sugars and imaged along the primary root. Roots of 5 individual seedlings were imaged at 25x magnification using the Leica SP5 confocal microscope. Several stacks per field were taken for each root and a 3D projection of the z-stack was obtained. Whole roots were then reconstructed in tiles. YFP emission was detected at 527 nm after excitation at 513 nm.

To localize expression in different LR developmental stages, 8 to 10 d-old seedlings of SnRK1α1 and bZIP63 were grown under long day conditions on ½ MS agar plates without sugars. The entire primary root was scanned for different stages of developing lateral roots (from stages II to emergence). Once located, several stacks per stage were taken and a 3D projection of the z-stack was obtained. Cell walls were counter stained with propidium iodide (PI) with a concentration of 10 µg/ml for 1min. For the detection of fluorescent signals from YFP and PI, different excitation and emission wavelengths were used. For PI fluorescence detection excitation and emission were at 570-670nm respectively and for YFP at 513-527nm.

Differential interference contrast imaging

Roots were cleared using an established protocol (2) introducing minor modifications. In detail, 5 d-old seedlings were treated with or without 4 h of uD, recovered in light for 16 h and cleared. Therefore, seedlings were first incubated at room temperature in a solution of 4% [(v/v)] HCl and 20% (v/v) methanol, followed by 7% (w/v) NaOH and 60% (v/v) ethanol for 15 min at a time. Plants were progressively rehydrated in 40, 20 and 10% ethanol changing the solutions every 5 min. The storage solution was 5% (v/v) ethanol in sterile water. Plants were placed on a glass slide with a solution of 50% (v/v) glycerol and topped with a cover slide. A Zeiss Axio Imager M1 microscope equipped with an AxioCamHR3_552 camera and DIC optics was used for imaging of the cleared roots.

Chromatin Immunoprecipitation coupled to PCR (ChIP-PCR)

We used 2 g root material of 10 d-old WT and *bZIP63*:YFP plants after treatment with 4 h of uD. The root tissue was incubated with cross-linking buffer (50 mM KH_2PO_4/K_2HPO_4 buffer, pH 5.8, 1% (v/v) formaldehyde) for 15 min under vacuum. Subsequently, samples were incubated in glycine buffer (50 mM KH_2PO_4/K_2HPO_4 buffer, pH 5.8, 0.3 M glycine) for 5 min under vacuum and washed three times with ice-cold water. Samples were dried with paper towels, frozen in liquid N_2 and either stored at -80˚C or ground using a pestle and mortar in liquid N_2. Nuclei extraction was performed at 4°C with pre-cooled equipment. The ground root material was re-suspended in 20 ml ice-cold extraction buffer (1 M hexylene glycol, 50 mM PIPES-KOH (pH7.2), 10 mM $MgCl_2$, 5 mM ß-

mercapto-ethanol, one tablet of Roche complete protease inhibitor cocktail tablets per 10 ml buffer) and the solution was filtered through a cell strainer into a clean beaker. Cold 25% (v/v) Triton X-100 (800 µl) was added dropwise to the nuclei extract, under stirring. This solution was incubated at 4°C for 15 min and the nuclei were isolated by density-gradient centrifugation using a 35% Percoll cushion in a pre-cooled centrifuge for 30 min at 2000 g. The supernatant was discarded, and the obtained nuclei pellet resuspended in gradient buffer (1 M hexylene glycol, 50 mM PIPES-KOH (pH 7.2), 10 mM $MgCl_2$, 5 mM ß-mercapto-ethanol). The nuclei were once again isolated by density gradient centrifugation using a 6 ml 35% Percoll cushion. The supernatant was discarded, the pellet re-suspended in 1 ml sonication buffer (10 mM Tris-HCl (pH 7.4), 1 mM EDTA (pH 8.0), 0.25% (w/v) SDS and Roche protease inhibitor) and incubated for 20 min. Another 0.5 ml of sonication buffer without SDS was added and mixed well before sonication. Chromatin was sheared using a Bioruptor device (Diagenode, Chicago, USA) for 3x 10 repetitions of 30 s at maximum power and 60 s of recovery. Chromatin was cleared by centrifugation for 5 min at 11,000 g and 4°C and stored at -80°C. For each IP 15 µg chromatin and 3 µg ChIP grade anti-GFP antibody (Abcam, Cambridge, UK) were used and incubated for 6 h at 4°C. An aliquot (70 µl) of protein G-coated magnetic beads (Invitrogen, Karlsruhe, Germany) suspended in ice-cold RIPAF buffer, supplemented with protease inhibitor (Roche, Mannheim, Germany) was added to each sample. Antibody-antigen binding was achieved during a 4 h incubation step at 4°C on a slowly rotating Intelli-Mixer. Beads were washed five times (with incubation for 5 min each time) with RIPAF buffer supplemented with protease inhibitor. Protein-DNA complexes were eluted using 30-70 µL elution buffer. Chromatin was incubated with 5 µl Proteinase K (Roche, Basel, Switzerland) overnight and purified using a DNA purification kit (Qiagen, Hilden, Germany) the following day. Precipitated DNA was quantified by qPCR using the oligonucleotide primers summarized in Supplementary Table S1. Data was normalized to DNA input (not-precipitated sample), which was quantified by employing *ACTIN8* (At1g49240) specific primers. Presented mean and SD values were calculated from three independent ChIP experiments that were performed on each of three independently prepared chromatin samples.

Chromatin-Immunoprecipitation DNA Sequencing (ChIPseq)

Ten d-old *bzip63* loss-of-function plants and the complementation line expressing *bZIP63*:YFP under control of the native promoter were treated with 4 h of uD. The roots were separated from the shoot and 10 g of root material was fixed in crosslinking buffer containing 1% (v/v) formaldehyde for 20 min (15 min in vacuum and 5 min without vacuum). Fixation was stopped by adding 2.5 ml glycine (1.25 M stock) and incubation for 5 min in vacuum. Chromatin extraction was done adopting an established protocol (3) introducing minor modifications. In detail, chromatin was sheared using a Covaris ultrasonicator (Covaris, Woburn, Massachusetts, USA) (Duty Cycle: 20%; Intensity: 5; Cycles per Burst: 200; Cycle time: 2 min). Incubation with antibody was done over-night and with protein-A agarose beads for 6 h. Purification of DNA after de-crosslinking was performed with a MinElute Reaction Cleanup Kit (Qiagen, Hilden, Germany). An aliquot (3 µg) of Anti-GFP (AbCam, Cambridge, UK) antibody was used for immuno-precipitation. ChIPseq libraries were prepared using a Library Preparation Kit (NEB, Massachusetts, USA) and the final concentration and size distribution of the libraries were tested with BioAnalyzer (Agilent High Sensitivity DNA Kit). Library preparation and Illumina high sequencing was carried out at Novogene Hongkong using the NEB Next Ultra II DNA Library Preparation Kit for Illumina (NEB, Massachusetts, USA). For ChIP-sequencing analysis, adapters were trimmed of from ChIPseq raw data and the reads were mapped to the A. thaliana (TAIR 10) genome with BWA-Burrows Wheeler Alignment (4) using default parameters. Mapped reads were sub sampled and peak calling for transcription factor binding was performed with MACS v2.1.1 (5). For regular peaks, the cut off value was kept at 9.00e+07 and q value at 0.01. For visualization, read density files containing peak information in bedgraph format were generated using the BEDTools v2.26.0 (6) and the Integrative Genomics Viewer (7). Genome annotations and pie charts to predict percentage of promoter TSS binding sites were analysed using ChIPSeek online web tool (8). bZIP63 target genes along with their gene descriptions from the TAIR database (TAIR10) are summarised in Supplementary Dataset S1.

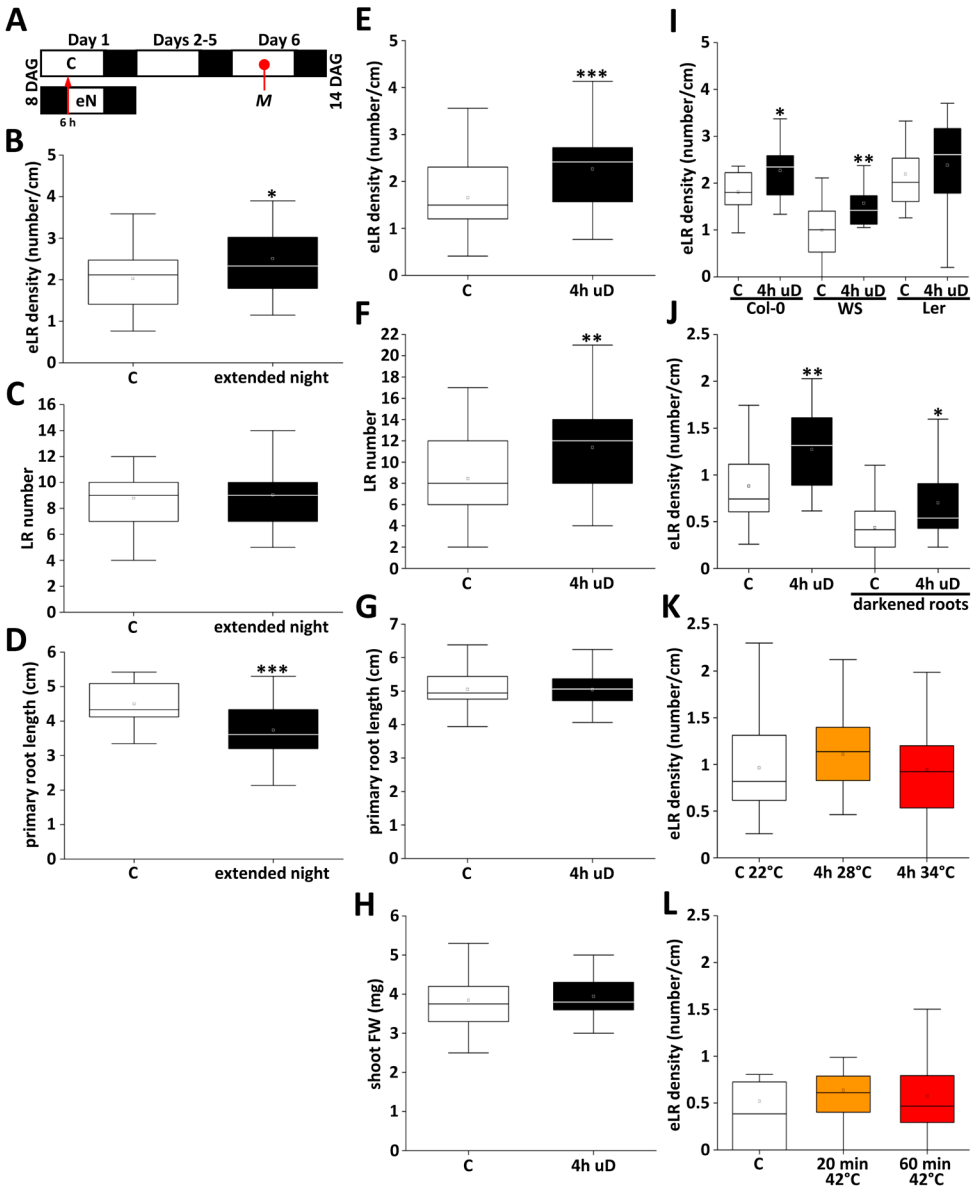

Fig. S1. Root plasticity in response to environmental changes. ***A***, Schematic representation on the experimental set-up studying extended night (eN) treatment. Arabidopsis (Col-O) seedlings were grown in a long day regime (16h light/8h dark, at 70 μmol m^{-2} s^{-1}) on solidified ½ MS media. After 8d, the night phase was extended once for 6h or the normal day/night regime maintained as control. Root parameters were assayed 14 DAG as given in ***B***, eLRD; ***C***, LR number and ***D***, primary root length. ***E-H***, Experiment studying uD as described in Fig. 1*E* comparing root parameters (***E***, eLRD; ***F***, LR number; ***G***, PR length) and fresh weight in the shoot (***H***). ***I***, Quantification of eLRD obtained upon uD as described in Fig. 1*E* analysing the Arabidopsis ecotypes Col-0, Ler and WS. ***J***, Root light perception does not affect the uD triggered LR response. Upon uD (as described in Fig. 1*E*) eLRD was quantified from roots that were exposed to light or darkened throughout the experiment, respectively. ***K***, Mild or (***L***) short-term severe heat stress was used as control treatment, to study specificity of the uD response. In both experiments 8d-old seedlings were pre-cultured at 22ºC (white box) before they were shifted to (***K***) a 4h unexpected mild heat stress (28°C, orange box or 34°C, red box) or to (***L***) severe heat (42ºC) for 20 (orange box) or 60 min (red box), respectively. After stress application plants recovered at 22°C for 6 days before eLRD was determined. Results are presented as box-plots. Statistically significant differences between control and treated samples were determined by Mann-Whitney`s U-test *p<0.05, **p<0.01, ***p<0.001. n=26 (***B-D***), n=45-50 (***E-H***), n=15-20 (***I***), n=24 (***J***), n=35-43 (***K***) or n=9 (***L***).

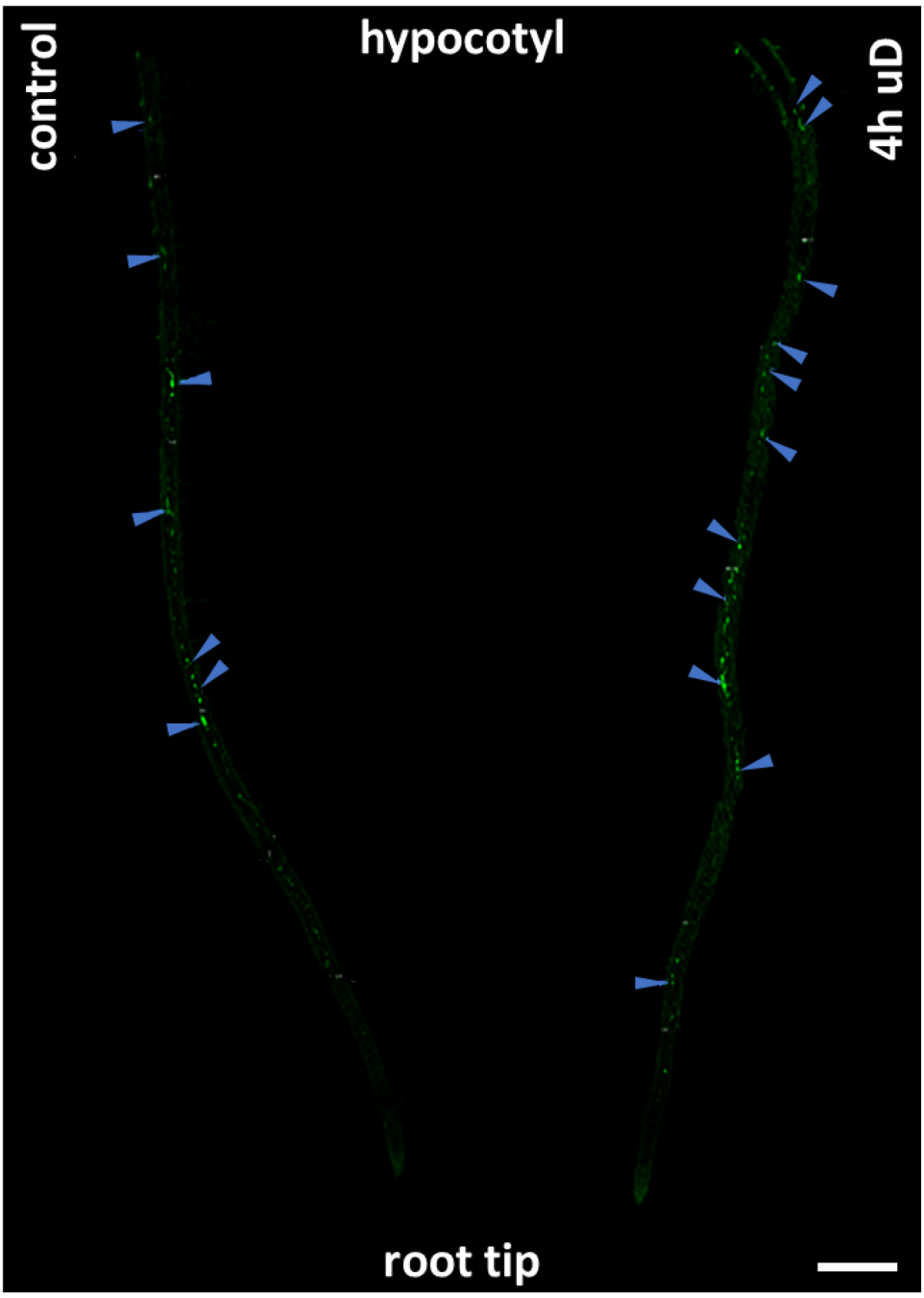

Fig. S2. Unexpected darkness leads to an increase in the number of cells showing expression of the early stage lateral root marker p*GATA23*::NLS-GFP (9). Mounted confocal microscopy images of representative WT roots under control conditions (left) or 4h of uD (right). GFP signals are marked by arrows. Scale bar: 500 µm.

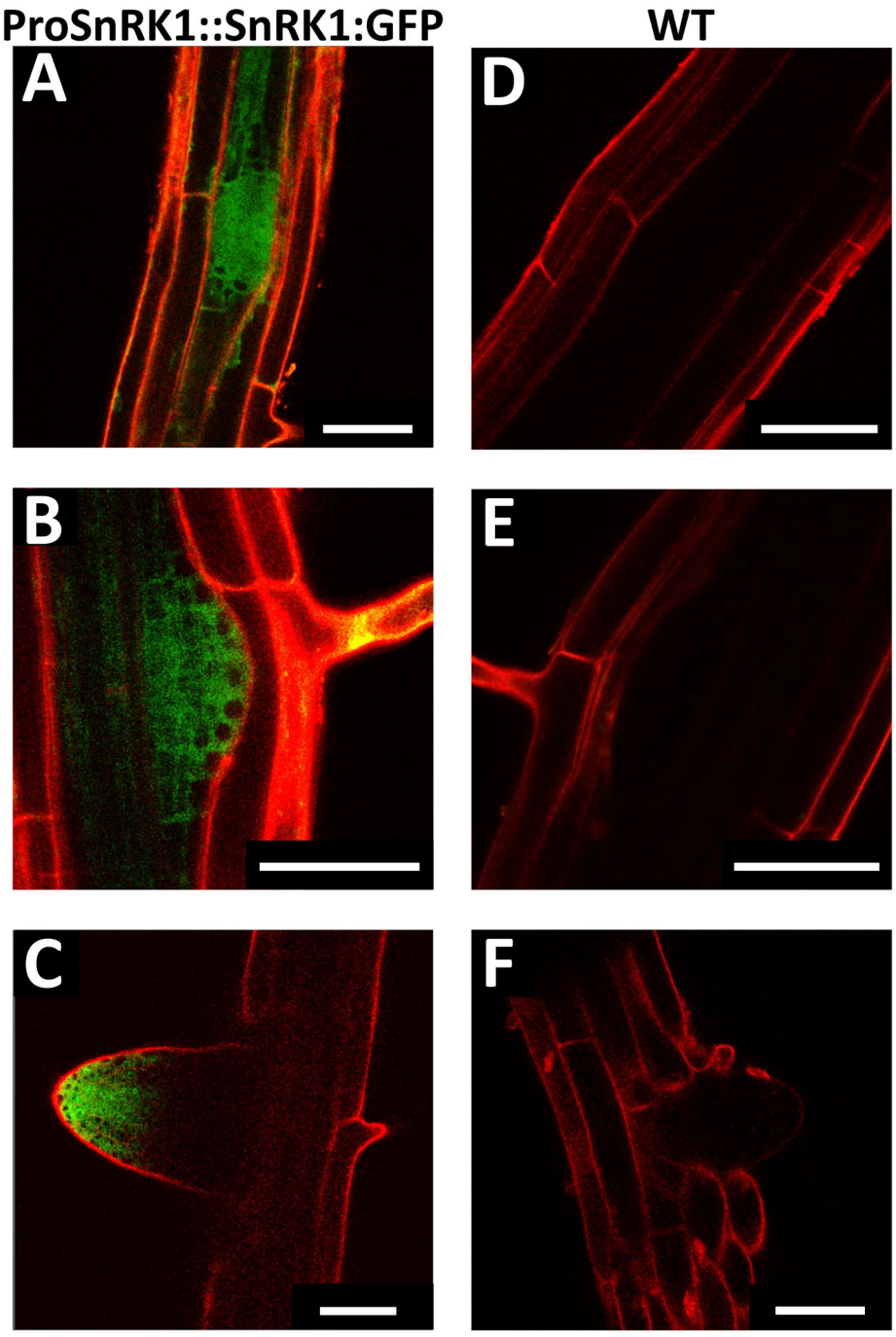

Fig. S3. Expression of SnRK1 in transgenic Arabidopsis seedlings. ***A***-***C***, SnRK1α1 expression in different stages of LR development studied by confocal microscopy, ***D***-***F***, WT controls do not show unspecific signals using the GFP excitation and emission settings used in ***A***-***F*.** Counterstaining with propidium iodide. Scale bar: 50 µm.

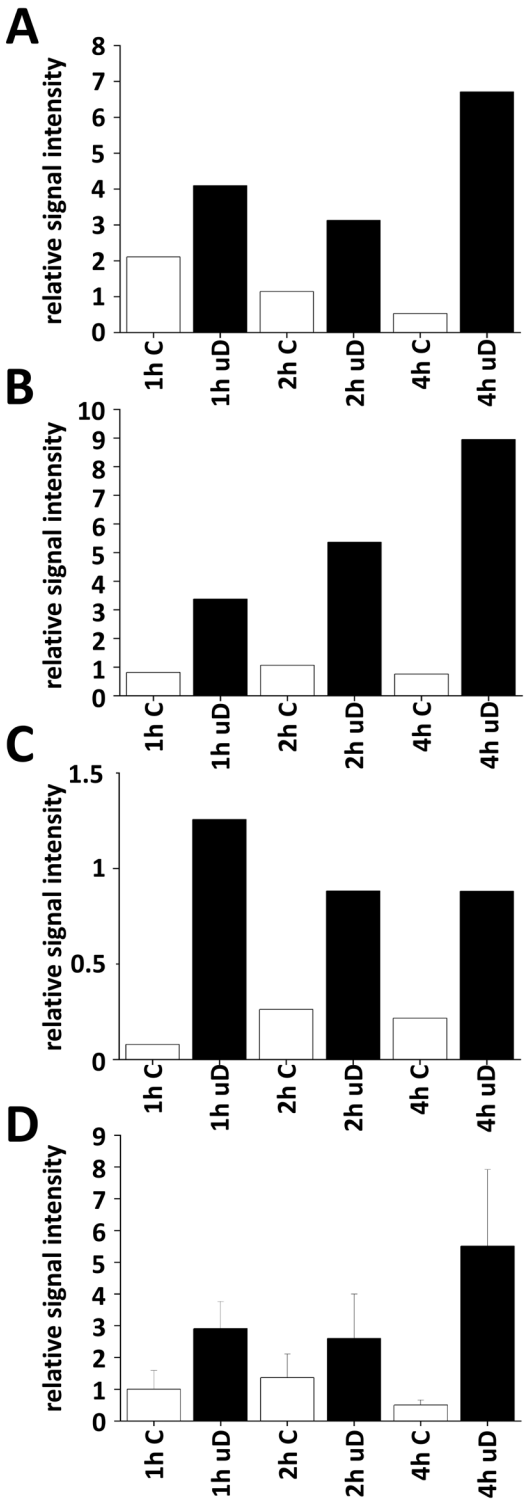

Fig. S4. Activity of SnRK1 in transgenic Arabidopsis seedlings. Nuclear ACC-ACC-GFP-HA-HA reporter protein was expressed in transgenic plants and its *in vivo* phosphorylation was assayed by immuno-detection using a P-dependent ACC-specific antibody (αP-ACC) and an αHA antibody for normalization. ***A***-***C***, Quantification of pACC signal relative to reporter abundance from 3 individual immunoblot experiments. ***D***, Presented are mean signal values +/- SEM from experiments given in ***A***-***C***).

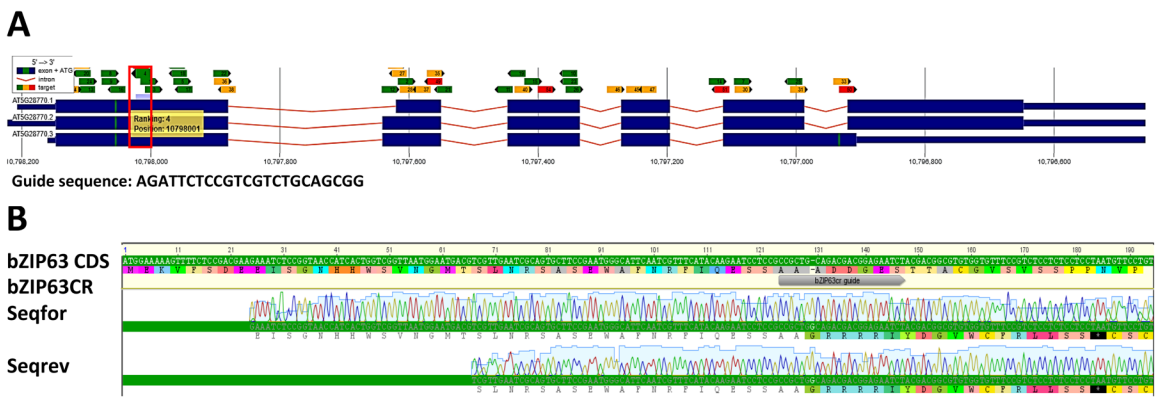

Fig. S5. A CRISPR/Cas9 derived *bzip63* knock-out line. ***A***, Schematic representation of the coding regions (exons given as blue boxes and introns as red lines) of the 3 known *bZIP63* isoforms. ChopChop (10) classified suited (green arrows) and less suited (yellow and red) CRISPR guide sequences in the *bZIP63* exon sequences. A red box indicates the position of the applied CRIPSR guide sequence within exon 1, which addresses all bZIP63 isoforms. ***B***, Molecular characterization of the Col-0 *bzip63*$_{CR}$ line. Sequencing reveals a G insertion in exon 1 of the *bZIP63* coding region, which is targeted by the CRISPR construct. This insertion leads to a frame-shift and consequently to a premature stop codon within exon1.

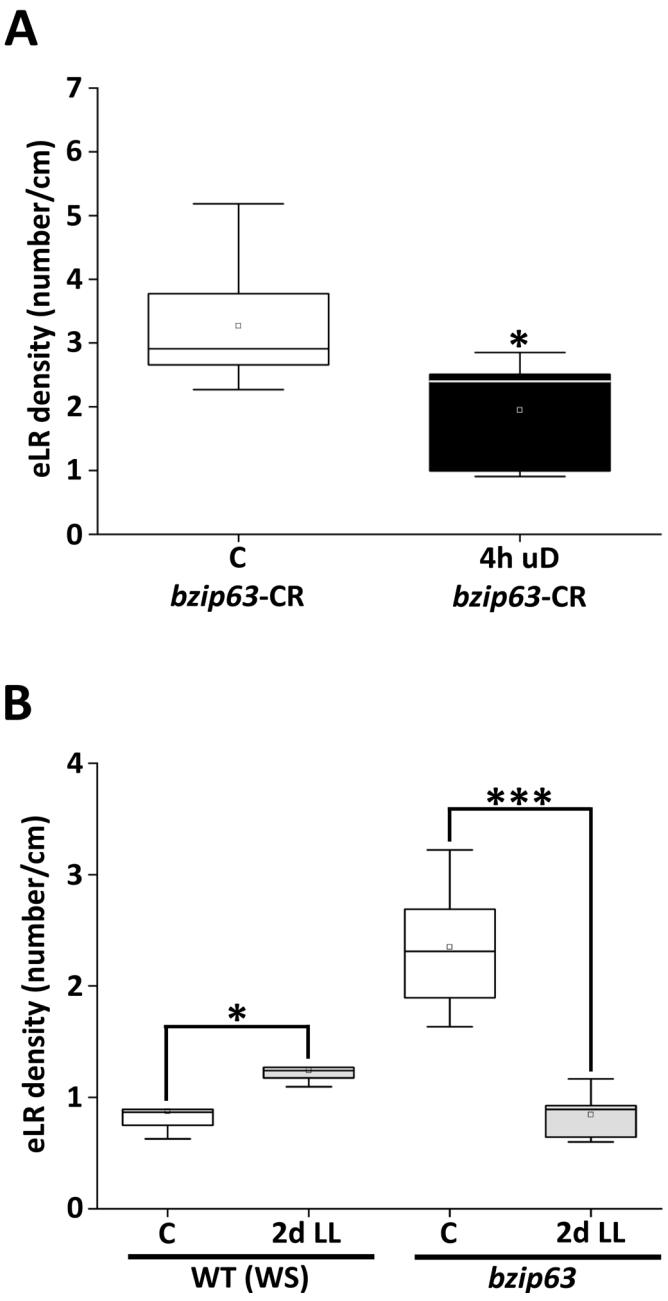

Fig. S6. *bzip63* knock-out lines are impaired in the low light- and unexpected darkness-induced enhanced lateral root density phenotype. ***A***, 8d-old, *bzip63*$_{CR}$ seedlings were grown on ½ MS media and subjected to control (white bars) or 4h uD conditions (black bars) (see Fig. 1*E*). eLRD was determined 14 DAG. ***B***, 8d-old, Arabidopsis WT (WS) and *bzip63* seedlings were grown on ½ MS media and subjected to control (white bars) or 24 h of low-light (grey bars) conditions (see Fig. 1*A*). eLRD was determined 14 DAG. Statistically significant differences between control and treated samples were determined by Mann-Whitney`s U-test, *p<0.05. n=5-10 each.

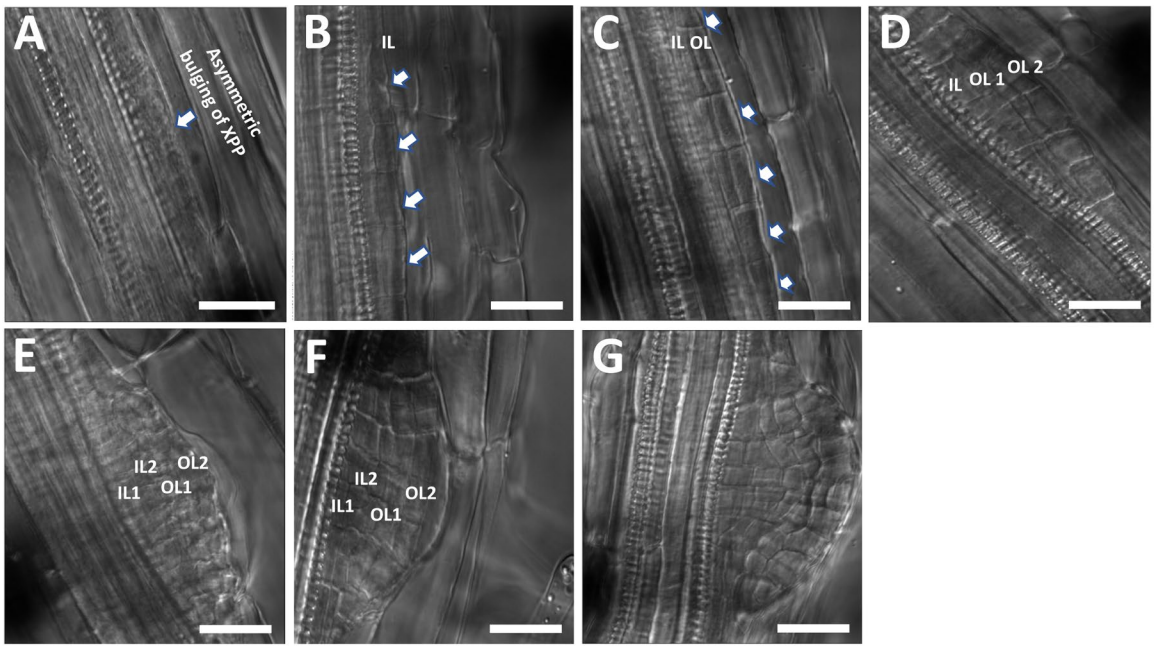

Fig. S7. Stages of lateral root development imaged by DIC microscopy (Differential Interference Contrast). ***A***, LR initiation stage where XPPs are activated and bulge before their first division. ***B***, Stage I: arrows indicate the first anticlinal division. ***C***, Stage II: arrows indicate periclinal division, leading to the formation of inner layer (IL) and outer layer (OL). ***D***, Stage III: second round of periclinal division in OL create a total of three layers. ***E***, Stage IV: third round of periclinal division creating 4 layers. ***F***, Stage V: anticlinal division resulting in four cell layers; initiation of complex reorganization of LR primordia. ***G***, Stage VI: each layer acquires cellular identity and forms epidermis, cortex, endodermis, and vasculature.

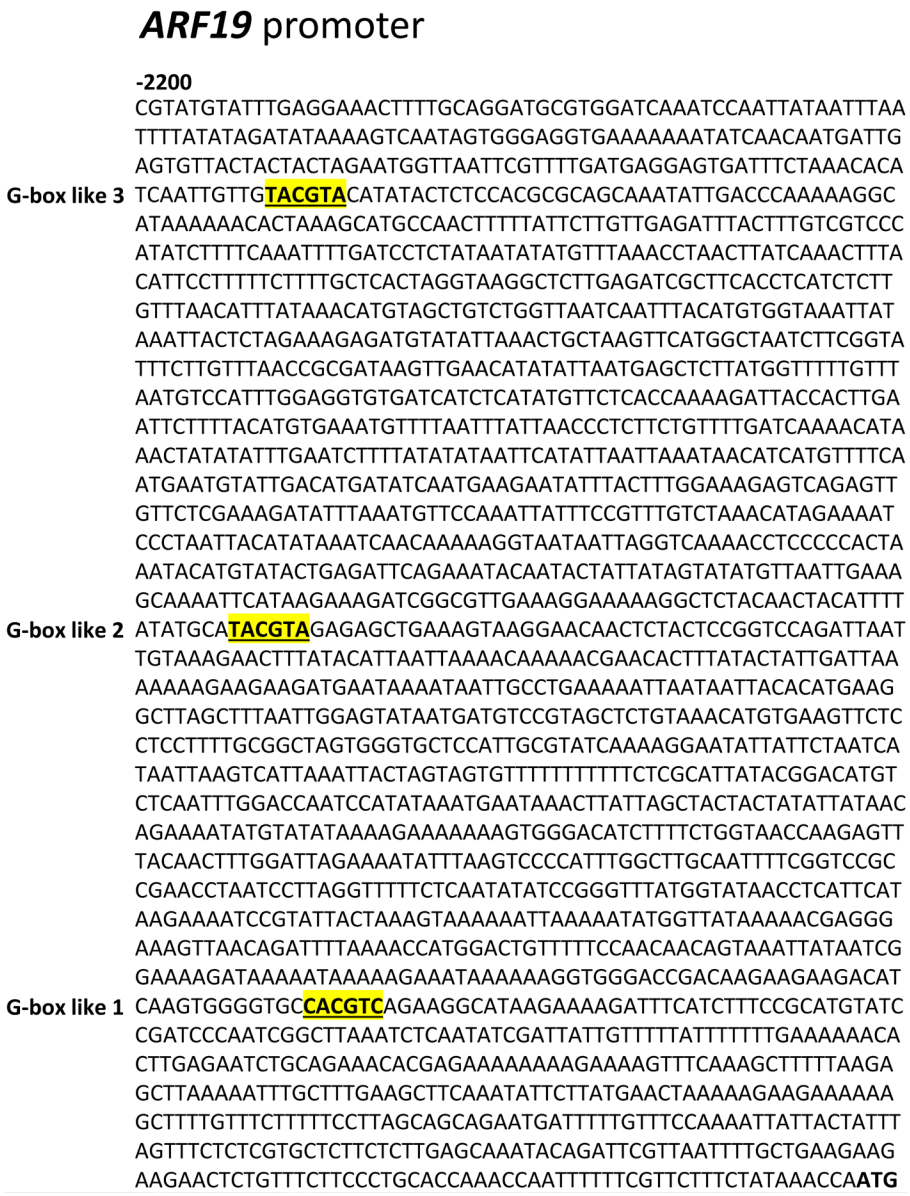

Fig. S8. Localization of G-box elements in the *ARF19* promoter. ATG translational start.

Table S1. List of plant lines and oligonucleotides used in this study

Plant lines

Wildtype/Transgenic Line	Characteristic	Reference
Wassilewskija (Ws)	Wildtype	
Columbia-0 (Col-0)	Wildtype	
Landsberg Erecta (Ler)	Wildtype	
snrk1.α1-3	Col-0, α1 subunit ko, GABI_579E09	(11)
snrk1.α2-2	Col-0, α2 subunit ko, snrk1α2-2 (WiscDsLox384F5)	(12)
SnRK1α1:GFP	SnRK1α1 N-terminal GFP fusion under the native promoter	(13)
AAC-reporter	Pro35S:NLS-ratAcc-GFP-2xHA	This study
GATA23:NLS-GFP	GATA23 N-terminal GFP fusion under the native promoter	(9)
bzip63	Ws, bZIP63 knockout (NASC ID: N700001)	(11)
bZIP63c	Ws, bZIP63 ko complemented with functional gene, N-terminal YFP fusion	(11)
bZIP63S/Ac	Ws, bZIP63 ko complemented with functional gene - S29/S294/S300 Ser to Ala exchanges, N-terminal YFP fusion	(11)
arf19	Col-0, ARF19 ko	(14)
bZIP63-CR	Col-0, CRISPR-Cas9 generated single point mutation in *bZIP63* gene	This study

Oligonucleotides

Gene	Forward (5`-3`)	Reverse (5`-3`)	Experiment
bZIP63	ATTGAGATTCTCCGTCGTCTGCAG	AAACCTGCAGACGACGGAGAATCT	CRISPR-Cas9 Gene editing
ARF19-GBox1	AAGACATCAAGTGGGGTGCC	TTGGGATCGGATACATGCGG	ChIP PCR
ARF19-GBox2	GGTCAAAACCTCCCCCACTA	GGACCGGAGTAGAGTTGTTCC	ChIP PCR
ARF19-GBox3	TCGTTTTGATGAGGAGTGATTTCT	GCTGCGCGTGGAGAGTATAT	ChIP PCR
Actin7	CGTTTCGCTTTCCTTAGTGTTAGCT	AGCGAACGGATCTAGAGACTCACCTT	ChIP PCR
Actin8	GGTTTTCCCCAGTGTTGTTG	CTCCATGTCATCCCAGTTGC	ChIP PCR
EF1A	ATGCCCCAGGACATCGTGATTTCAT	TTGGCGGCACCCTTAGCTGGATCA	qRT-PCR
ASN1	CACGTGTACGGCTCTAAAGCA	GACCAGCTGTTTCCACGTGTT	qRT-PCR
ARF19	AGCTGGAGATAGGCCAAGCC	TCTGTGCGTCCTTCATCCCA	qRT-PCR
bZIP63	GAAGAAATCTCCGGTAACCATCAC	GATTCTCCGTCGTCTGCAGC	qRT-PCR

SI References

1. J. Schindelin, *et al.*, Fiji: An open-source platform for biological-image analysis. *Nat. Methods* **9**, 676–682 (2012).
2. J. E. J. E. Malamy, P. N. P. N. Benfey, Organization and cell differentiation in lateral roots of Arabidopsis thaliana. *Development* **124**, 33–44 (1997).
3. K. Kaufmann, *et al.*, Chromatin immunoprecipitation (ChIP) of plant transcription factors followed by sequencing (ChIP-SEQ) or hybridization to whole genome arrays (ChIP-CHIP). *Nat. Protoc.* **5**, 457–472 (2010).
4. H. Li, R. Durbin, Fast and accurate long-read alignment with Burrows–Wheeler transform. *Bioinformatics* **26**, 589–595 (2010).
5. Y. Zhang, *et al.*, Model-based analysis of ChIP-Seq (MACS). *Genome Biol.* **9** (2008).
6. A. R. Quinlan, I. M. Hall, BEDTools: a flexible suite of utilities for comparing genomic features. *Bioinformatics* **26**, 841–842 (2010).
7. J. T. Robinson, *et al.*, Integrative genomics viewer. *Nat. Biotechnol.* **29**, 24–26 (2011).
8. T. W. Chen, *et al.*, ChIPseek, a web-based analysis tool for ChIP data. *BMC Genomics* **15**, 539 (2014).
9. B. De Rybel, *et al.*, A novel Aux/IAA28 signaling cascade activates GATA23-dependent specification of lateral root founder cell identity. *Curr. Biol.* **20**, 1697–1706 (2010).
10. K. Labun, *et al.*, CHOPCHOP v3: Expanding the CRISPR web toolbox beyond genome editing. *Nucleic Acids Res.* **47**, W171–W174 (2019).
11. A. Mair, *et al.*, SnRK1-triggered switch of bZIP63 dimerization mediates the low-energy response in plants. *Elife* **4**, e05828 (2015).
12. B. Belda-Palazón, *et al.*, A dual function of SnRK2 kinases in the regulation of SnRK1 and plant growth. *Nat. plants* **6**, 1345–1353 (2020).
13. M. Bitrián, *et al.*, BAC-recombineering for studying plant gene regulation: developmental control and cellular localization of SnRK1 kinase subunits. *Plant J* **65**, 829–842 (2011).
14. Y. Okushima, H. Fukaki, M. Onoda, A. Theologis, M. Tasaka, ARF7 and ARF19 Regulate Lateral Root Formation via Direct Activation of LBD/ASL Genes in Arabidopsis . *Plant Cell* **19**, 118–130 (2007).